Electronic Supplementary Material (ESI) for Journal of Materials Chemistry A.

Electronic Supplementary Information

Nitrogen-Enriched and Hierarchically Porous Carbon Macro-Spheres - Ideal for Large-Scale CO_2 Capture

Bingjun Zhu, Kaixi Li, Jingjing Liu, Hao Liu, Chenggong Sun, Colin Snape, Zhengxiao Guo*

1. Optimizing the spherical shape

The roundness of the spherical head and the length of the tail depend on the concentration and viscosity of the polymer solution. With a higher concentration and viscosity, that is, the initial polymer solution is diluted with less DMSO, it tends to produce a polymer sphere with an elliptical head with a thick long tail. In contrast, with a lower concentration and viscosity, it tends to produce a sphere with a flattened head but a short and slim tail. The shape of the spheres is also influenced by the distance between the nozzle and the water surface. A shorter distance may result in an incomplete formation of spherical shape due to insufficient time before the polymer solution drop enters the water bath. On the contrary, too long a distance may cause severe distortion of the spherical head, due to increased impact between the drop and the water bath surface. Distances of 10, 15, 20 and 25 cm were assessed and 15 cm was identified as appropriate to produce a relatively spherical geometry in the current case. In addition, the molar ratio of acrylamide/acrylonitrile also influences the shape of the sphere. With the same total weight (9.1 g) of monomers in the copolymerization reaction, while the polymer spheres prepared with the ratio of 1:3.3 give the best spherical shape, those prepared with 0:1 and 1:10.9 exhibit certain degrees of flattened heads, similar to the situation where the polymer solution is over diluted. Acrylamide possesses a higher molecular weight (71 g mol^{-1}) than that of acrylonitrile (53 g mol^{-1}). The increasing acrylamide content raises the average molecular weight of the resulting copolymer and subsequently increases the viscosity of the polymer solution. However, acrylamide is a water-soluble monomer so that increasing acrylamide content also raises the hydrophilicity of the copolymer. Hence, the spheres prepared with the ratio of 1:1.5 partially dissolve in the water bath and also tend to agglomerate, so are difficult to separate without damaging the spheres. **Figure S1** shows uniformity and relative size of the polymer spheres, compared with that of a penny (~ 20 mm in diameter).

Figure S1: A pile of polymer spheres compare with the size of a penny, showing good uniformity and sphericity of the sphere.

2. Mechanism of Oxidation

Figure S2 schematically illustrates the mechanisms of the cyclization reactions of polyacrylonitrile, where the reaction is initiated by oxygen in the air, and that of poly(acrylonitrile-co-acrylamide), which can be initiated by its amide groups without oxygen.

Both can occur simultaneously when the copolymer is oxidized in the air. After the activation reaction, the intensities of both peaks are greatly reduced due to further loss of nitrogen content and regular pyridinic structure due to chemical attack by KOH.

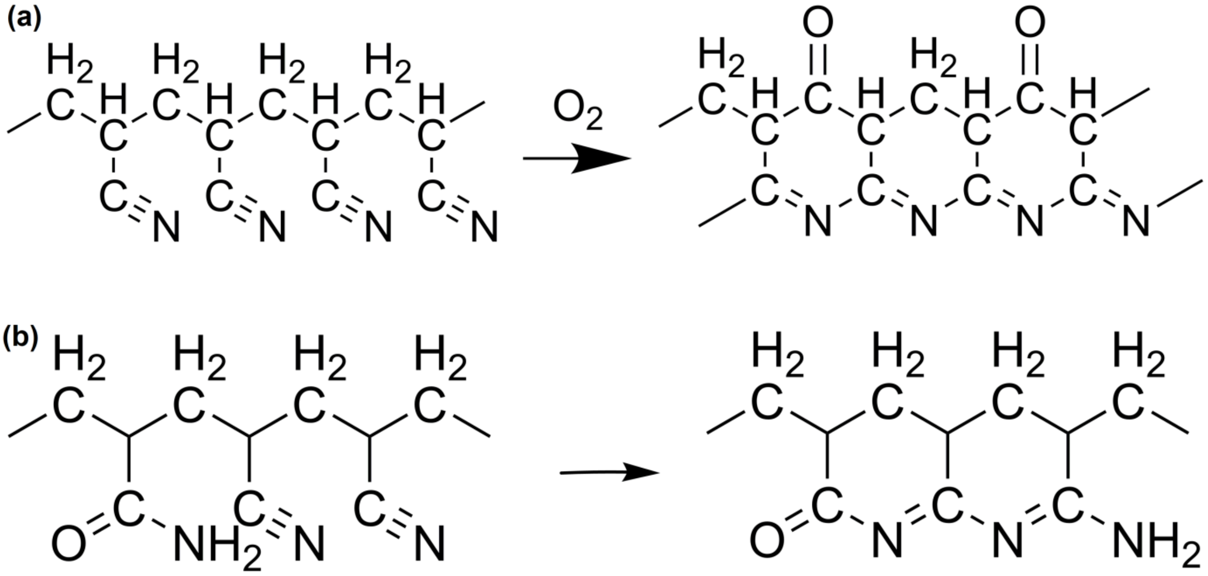

Figure S2: Mechanisms of **(a)** oxidation of polyacrylonitrile with the participation of O_2 and **(b)** cyclization of poly(acrylonitrile-co-acrylamide) without the participation of O_2.[1]

3. Mechanism of Activation

Below 700 °C, the mechanism is mainly based on the dehydration reaction of KOH and the reduction reactions between dehydration products and carbon (**Equation 1-3**). Potassium carbonate is formed as a by-product (**Equation 4**):[2]

$2KOH \rightarrow K_2O + H_2O$ (1) $C + H_2O \rightarrow CO + H_2$ (2)

$CO + H_2O \rightarrow CO_2 + H_2$ (3) $CO_2 + K_2O \rightarrow K_2CO_3$ (4)

Conversely, above 700 °C, the decomposition of potassium carbonate (**Equation 5**) generates potassium oxide and carbon dioxide, both of which take part in further reduction reactions with carbon (**Equation 6-8**):[3]

$K_2CO_3 \rightarrow CO_2 + K_2O$ (5) $CO_2 + C \rightarrow 2CO$ (6)

$K_2CO_3 + 2C \rightarrow 2K + 3CO$ (7) $C + K_2O \rightarrow 2K + CO$ (8)

These reactions above 700 °C play an important role to further enlarge the surface area and pore volume. However, they also widen the pore size range and alter the pore size distribution.

4. Residual Potassium

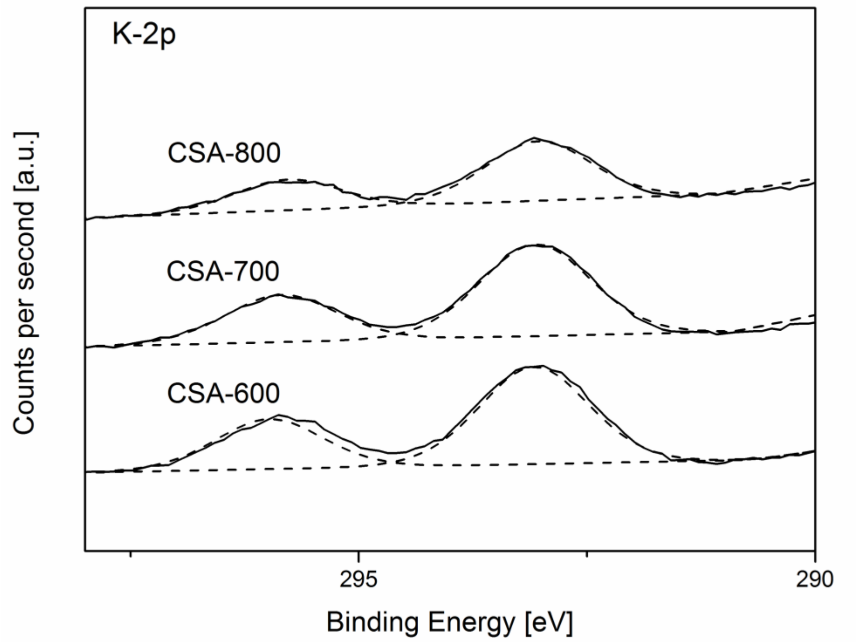

Figure S3: K-2p XPS spectra of activated carbon spheres.

Besides the nitrogen content, another interesting observation is the residual potassium content after the samples were washed by distilled water. All activated carbon spheres possess a certain amount of residual potassium content. **Figure S3** shows that all K-2p spectra have two major peaks centered at 295.9 (K-2p1/2) and 293.0 eV (K-2p3/2). It indicates the valence of the potassium content is +1. An earlier study suggests that it implies the potassium content may be intercalated into the carbon structure in the form of extra-framework cations.[4] The author argues that the intercalation of potassium cations improves the CO_2 adsorption performance by enhancing the electrostatic interaction between CO_2 gas molecules and carbon structures.

5. Micropore size distribution by CO_2 sorption

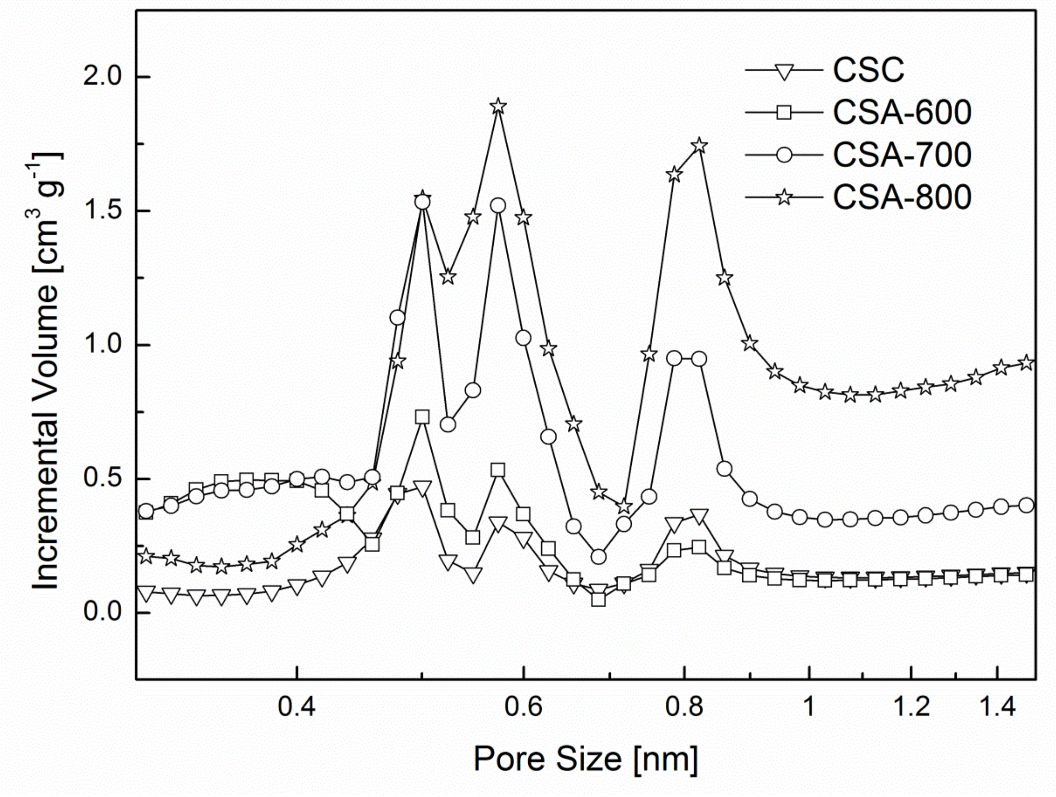

Figure S4: Micropore size distribution (Log).

Figure S4 shows the micropore size distribution of carbon spheres analyzed by CO_2 sorption at 0 °C, using the CO_2-on-Carbon@273K NLDFT model. Three major peaks are noted at 0.5, 0.6 and 0.8 nm, respectively. It is clear that the intensities of these peaks increase with the activation temperature from 600 to 800 °C. This figure provides additional information of pore size distribution below 1 nm. It has been discussed in the literature that there exists diffusion limitation of N_2 molecules in the ultra-micropores of activated carbon and thus N_2 sorption is not accurate for ultra-micropore analysis.[5] However, compared with **Figure 3a**, where pore size distribution is analyzed by N_2 sorption at -196 °C, some information of pore size distribution is "lost" between 1 to 1.5 nm for CO_2 sorption. Similar findings have been observed earlier.[5] This is attributed to the limitation of incomplete gas filling of pores above 1 nm for CO_2 sorption analysis up to atmospheric pressure.[6] The above results further confirm the complementary characteristics of N_2 and CO_2 probes for porosity analysis.

6. Macropore size distribution

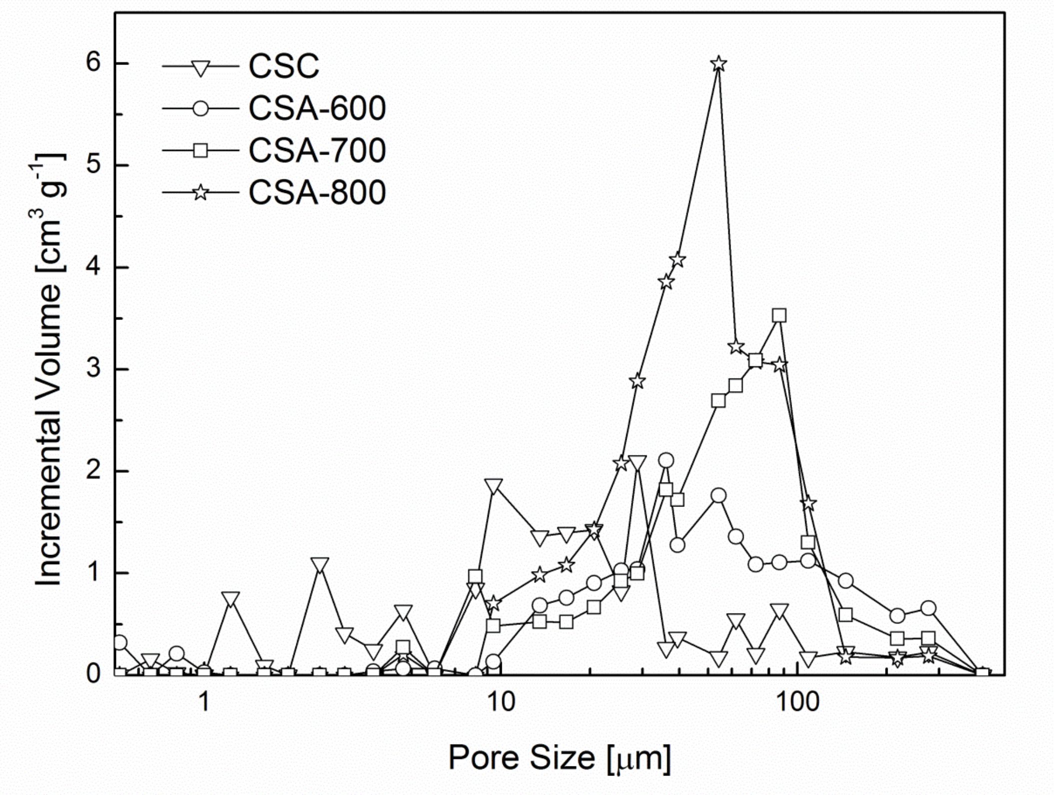

Figure S5: Macropore size distribution (Log).

Figure S5 provides additional information of pore size distribution in the macropore range (up to 421 μm), using mercury porosimetry. In comparison with the SEM images in **Figure 1**, this figure shows clearly that the macropores are mainly distributed between 10 to 100 μm, with some very large macropores between 200-400μm, for all three types of samples; the former range corresponds to pores in the mantle region and the latter the inner region. It may also be noted that the pore volume "V_{Hg}", derived from Mercury Porosimetry, are larger than "V_{N2}", derived from N_2 sorption isotherms. This is because the analysis for N_2 sorption is designed for assessement of micro-/meso- pores, based on the Kelvin Equation at $P/P_0 = 0.99$, where the corresponding maximum pore size is ~ 190 nm. In summary, this complementary figure confirms that for the accurate assessment of macro-pores, mercury porosimetry is the appropriate technique.

7. References

1 H. Fu, *Carbon Fiber and Graphite Fiber*, Chemical Industry Press, Beijing, China **2010**, pp. 145-146.

2 J. Romanos, M. Beckner, T. Rash, L. Firlej, B. Kuchta, P. Yu, G. Suppes, C. Wexler, P. Pfeifer, *Nanotechnology* 2012, **23**, doi:10.1088/0957-4484/23/1/015401.

3 J. C. Wang, S. Kaskel, J. Mater. Chem., 2012, **22**, 23710-23725.

4 Y. F. Zhao, X. Liu, K. X. Yao, L. Zhao, Y. Han, Chem. Mater. 2012, **24**, 4725-4734.

5 J. Jagiello, M Thommes, Carbon, 2004, **42**, 1227-1232.

6 P. I. Ravikovitch, A. Vishnyakov, R. Russo, A. V. Neimark, Langmuir, 2000, **16**, 2311-2320.